Magnetism at Single Isolated Iron Atoms Implanted in Graphite

R. Sielemann,[1] Y. Kobayashi,[2] Y. Yoshida,[3] H. P. Gunnlaugsson,[4] and G. Weyer[4]

[1]*Hahn-Meitner-Institut Berlin GmbH, 14109 Berlin, Germany*
[2]*Institute of Physical and Chemical Research (RIKEN), Saitama, Japan*
[3]*Shizuoka Institute of Science and Technology, Shizuoka 437-8555, Japan*
[4]*Department of Physics and Astronomy, University of Aarhus, DK-8000 Aarhus, Denmark*

(Received 12 March 2008; published 26 September 2008)

Mössbauer spectra obtained after implantation of ^{57}Fe into highly oriented pyrolytic graphite (HOPG) show a combined magnetic and quadrupole interaction with a magnetic hyperfine field $B_{\mathrm{hf}} = 32.6$ T at 14 K. Though magnetic effects in nominally diamagnetic HOPG have been reported recently, no experiment has previously shown the existence of magnetism at the atomic scale. The results suggest that magnetic ordering occurs by coupling of the Fe magnetic moment to structural and/or electronic magnetic defects induced by the probe atoms' implantation damage.

DOI: 10.1103/PhysRevLett.101.137206 PACS numbers: 75.50.Dd, 61.72.up, 76.80.+y, 81.05.Uw

Magnetism in solids generally requires the presence of magnetic ions which by some kind of exchange coupling may form an ordered magnetic phase. There are strong efforts to develop materials in which the magnetic ions constitute only a minor fraction to produce materials with new functionalities. Driving forces for this research are interest in the fundamental physics of magnetism as well as the quest for possible applications, e.g., for spintronics or towards the development of lighter magnetic materials. Diluted magnetic semiconductors (DMS) containing 3d magnetic ions in the percent range form such a class of materials. However, experimental evidence for magnetism is often contradictory, and theory describing the underlying mechanisms is still under discussion [1]. Even more attractive would be materials with still lower magnetic ion concentrations or no such ions at all which, nevertheless, might become magnetic under certain conditions. Carbon based materials, e.g., have been reported to show magnetic properties in specific circumstances [2,3]. A striking example reports magnetism in graphite apparently induced by proton irradiation [3]. Topological defects, disordering of the electronic system, or ferromagnetic inclusion-induced magnetism were proposed as possibly related to the observed phenomena [4–6]. Another class of materials with similar findings comprises certain oxides like, e.g., HfO_2 [7,8]. It is clear that any possible route evoking magnetism in these materials is of considerable interest.

In this Letter, we present experiments which probe magnetism in graphite at the atomic scale, an important feature missing as yet in all former experiments reporting mostly average magnetization. We correlate single Fe ions with a high concentration of point defects and disorder created by implanting ^{57}Fe probe atoms and perform Mössbauer spectroscopy (MS) on these probes. Several Mössbauer studies with implanted ^{57}Co in graphite have been reported, mostly performed at and above room temperature, see Ref. [9]. The special MS method employed is the In-Beam Mössbauer Spectroscopy (IBMS), which combines Coulomb excitation of the Mössbauer active state with the recoil implantation of the excited atom. This technique exploits the high sensitivity of MS and allows to work at low and high temperatures. By measuring quadrupole and magnetic interactions simultaneously, access to both structural and magnetic properties is obtained in the probes' atomically local environment. Spectra may be composed of single lines, doublets, and sextets depending on whether cubic symmetry sites, sites with quadrupole, or sites with magnetic interactions are observed, see Refs. [10–12].

The present experiments were performed at the heavy ion accelerator of the Hahn-Meitner-Institut (HMI) in Berlin. A pulsed beam (pulse width 5 ns, repetition rate 1 MHz) of Ar ions of energy 110 MeV is scattered at a ^{57}Fe metallic foil. Whereas the unscattered primary beam does not hit the graphite sample, scattered ^{57}Fe nuclei are expelled from the foil and implanted into the sample material positioned behind the foil to the right and left of the Ar beam. A fraction of the scattered nuclei is Coulomb excited to the 14.4 keV Mössbauer level. It decays with a lifetime of 140 ns, and the emitted 14.4 keV radiation is detected in the time intervals between pulses. The Coulomb excitation process in a ^{57}Fe foil of 3 mg/cm^2 leads to implantation of single Fe atoms dispersed over a depth of 0 to about 14 μm (energies up to 90 MeV) with a flat maximum around 40°. The total number of Fe atoms is below 10^{10} leading to concentrations between 10^{13} and 10^{16} cm^{-3}, thus ensuring together with a measuring time interval of about 1 μs after implantation that no Fe clustering can take place. The Fe atoms in flight carry charges up to 20^+ but will be neutralized within ps in the graphite matrix long before the MS starts. Additional details of the implantation conditions can be found in [13].

Three different types of material were used: (i) Highly Oriented Pyrolytic Graphite (HOPG) from Panasonic Co.

(Japan), (ii) HOPG from Advanced Ceramics (USA), and (iii) high purity polycrystalline commercial graphite material. Two samples with dimensions 20×35 mm^2 and 1 mm thickness were mounted vertically on the cold finger of a cryostat, the surface normal forming an angle of 10° with the beam direction. Two gas-filled resonance detectors [14] were positioned almost 90° to the beam direction, i.e., at an angle of 10° to the surface planes. These counters were equipped with electrodes made from stainless steel enriched in ^{57}Fe. For the HOPG samples, the crystallographic c axis is directed along the surface normal; there is no long range ordering, however, in the surface plane. The spectra of ^{57}Fe in HOPG were taken between 14 K and room-temperature (RT); to achieve the low temperatures, the whole assembly was surrounded by a heat shield.

Figure 1 shows spectra taken with sample (i) at 3 temperatures between 14 and 200 K. At 100 and 200 K, the spectra are composed of several lines around zero velocity. At 14 K, however, there are additional spectral components at large velocities indicating a magnetic state. Analysis of the data was started with the spectra at 100 and 200 K where no magnetic splitting is present. An ansatz with 2 quadrupole split (QS) doublets $D1$ and $D2$ and one singlet $S1$ is needed to describe the data consistently. The evaluation of the quadrupole-split spectra of the HOPG samples allows determining the direction of the principle axis of the electric field gradient (EFG), z, with respect to the crystal's

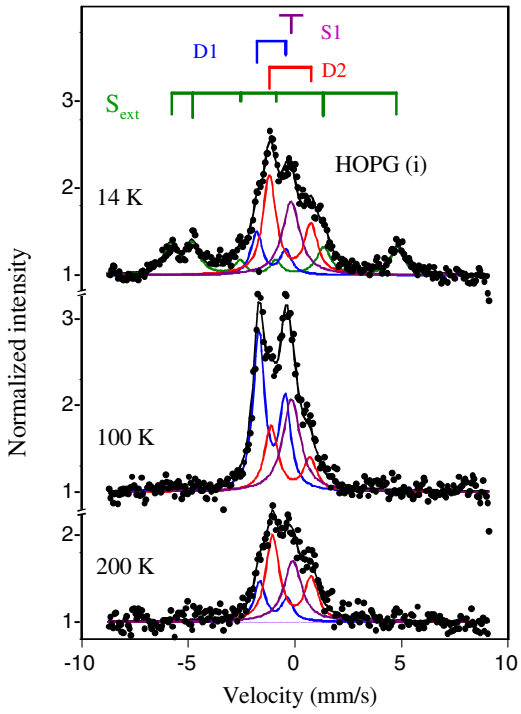

FIG. 1 (color online). Mössbauer spectra of ^{57}Fe after implantation in graphite sample sample: HOPG (i) at the temperatures indicated. Fitted components S_{ext}, $D1$, $D2$, and $S1$ given as bars on top with relative intensities of the contributing lines.

c axis. For both $D1$ and $D2$, a strongly asymmetric doublet with an intensity ratio close to 3:5 (high velocity to low velocity peak) is needed for the fit at all temperatures. This intensity ratio calls for a solution with z parallel to c and a positive sign for the QS. The assignment is additionally proved by the measurement of the combined interaction for $D1$ (see below). In this principal axes system of the EFG, the angle of observation of the 14.4 keV γ-rays is 80(5)° to the $z(c)$ axis. Doublet ($D1$) has a high isomer shift, IS $= +0.93$ mm/s (low electron density), and doublet ($D2$) has small shift, IS $= +0.06$ mm/s, all values given at 300 K, see Table I. The singlet ($S1$) has IS $= +0.02$ mm/s. The quadrupole splittings are shown in Fig. 4. The asymmetry parameters η remain undetermined.

To analyze the spectrum at 14 K with a magnetic splitting (S_{ext}), we tentatively subtracted the data taken at 100 K (not shown). A spectrum with 6 lines of unequal spacing indicating combined magnetic and quadrupolar interaction showed up, and $D1$ at $+0.93$ mm/s appeared with negative intensity, the rest of the spectrum practically cancelled. This shows that S_{ext} forms at the expense of $D1$ when the temperature is lowered. S_{ext} can be successfully analyzed without recourse to $D1$: The IS amounts to $+0.89$ mm/s, and QS is $+1.21$ mm/s; the sign of QS is uniquely determined from the positions of the sextet lines, and the orientation is given as $z \| c$, see also above. In addition, a magnetic hyperfine field, B_{hf}, is determined also as parallel to the principal z-axis (and therefore c) with a value of $B_{hf} = 32.6$ T. The IS and QS are identical with the values of $D1$ within error limits confirming that a transition from this doublet to S_{ext} is observed without change of the structural parameters.

A further experiment in the low temperature regime (40 K) was performed with HOPG sample (ii) to obtain

TABLE I. Fit parameters of the components S_{ext}, $D1$, $D2$, $S1$ for Fe implanted in different graphite samples from simultaneous analysis. IS is always given at 300 K obtained from the respective measuring temperature with correction for SOD assuming the Debye temperatures (θ_D) given relative to center of the spectrum of α-Fe at RT. QS for $D1$ and $D2$ is given as function of temperature in Fig. 4. The linewidth (Γ) is given as the Lorentzian broadening (FWHM) having subtracted the detector linewidth. For the sextet, it is the average of all pairs.

	S_{ext}	$D1$	$D2$	$S1$
B_{hf} (14 K) (T)	32.6(3)			
B_{hf} (40 K) (T)	29.8(8)			
IS (mm/s)	0.89(3)	0.93(2)	0.06(2)	0.02(3)
θ_D (K)[a]	170	170	300	300
QS (mm/s)	1.21(6)	Fig. 4	Fig. 4	···
Γ (mm/s)	0.66(4)	0.55(3)	0.71(4)	0.91(5)
$I(+)/I(-)$[b]	0.63(fix)	0.63(3)	0.67(2)	···

[a]Not included as a fitting variable, estimated from the intensity of the respective component as function of temperature.
[b]Intensity ratio high velocity peak to low velocity peak.

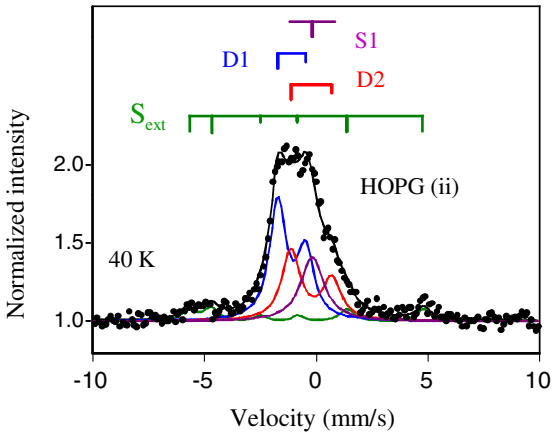

FIG. 2 (color online). Implantation in sample: HOPG (ii).

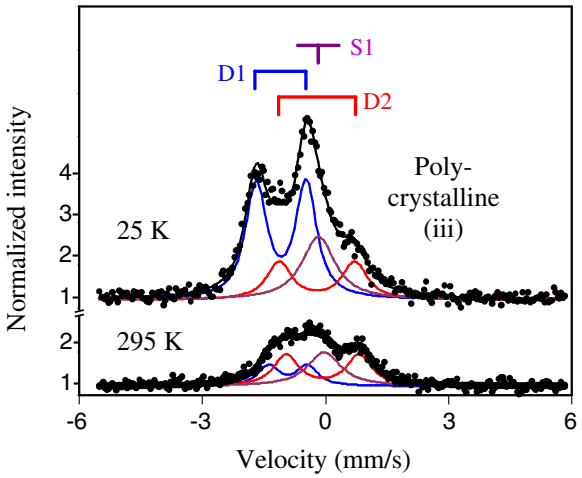

FIG. 3 (color online). Implantation in sample: Polycrystalline (iii). Notice the symmetric doublets in contrast to Figs. 1 and 2.

more details on the onset of the magnetic splitting, Fig. 2. It is seen that, compared to the 14 K spectrum, the fraction of the magnetic component strongly decreases while simultaneously that of the doublet $D1$ increases. Along with that behavior, B_{hf} decreases to 29.8 T; the magnetic hyperfine field is strongly temperature dependent.

Another set of data was taken with poly-graphite [sample (iii)] at 25 and 292 K, see Fig. 3. There is no indication of magnetic splitting in these spectra. For the analysis, we used the same ansatz given above (2 doublets, 1 singlet, no magnetic splitting), this time, however, with symmetric doublets as should be appropriate for polycrystalline material if a possible Goldankii-Karyagin effect [15] is not too strong. Again, this ansatz fits the data well, see Fig. 3 and also Ref. [16]. Following the analysis with individual fits to all spectra, we applied a simultaneous fitting procedure. These fits are displayed together with the spectra in Figs. 1–3, showing that the various materials can be fitted with one unique decomposition of the spectral components. The relative fractions are shown in Fig. 4, and the parameters of the simultaneous fitting are given in Table I. The large IS $= +0.93$ mm/s of $D1$ allows an unequivocal assignment to ferrous, high-spin Fe ions, Fe^{II}. The measured QS and B_{hf} values are also typical for this electronic configuration [17]. The low electron density points to a lattice position interstitial between graphene sheets. Similar large IS were measured and calculated for interstitial Fe in several semiconductors [18]. $D2$ and $S1$ both have IS close to zero. Though not very specific in itself, these relatively larger IS values make positions within or close to the graphene sheets more likely.

How can the available information for $D1$ be related to the observed magnetism? Elastic-Recoil-Detection-Analysis (ERDA) after one of the experiments [sample (ii)] revealed 8×10^{-4} atomic concentration of oxygen, about 10^{-3} of hydrogen, and 2×10^{-5} of Fe [19]. These concentrations are not in a range to directly influence collective magnetic properties. However, the salient feature of the experiment is that each implanted probe induces a damage cascade leaving defects in the concentration range of 1% around the final lattice position [20]. A defect density in the percent range was recently calculated sufficient to induce magnetic ordering in certain oxides [21,22]. For graphite [4], such a scenario was also suggested. The authors showed that intrinsic defects and certain impurity atoms carry magnetic moments in these materials and that a realistic exchange interaction can be found leading to magnetic ordering. In addition to or in combination with

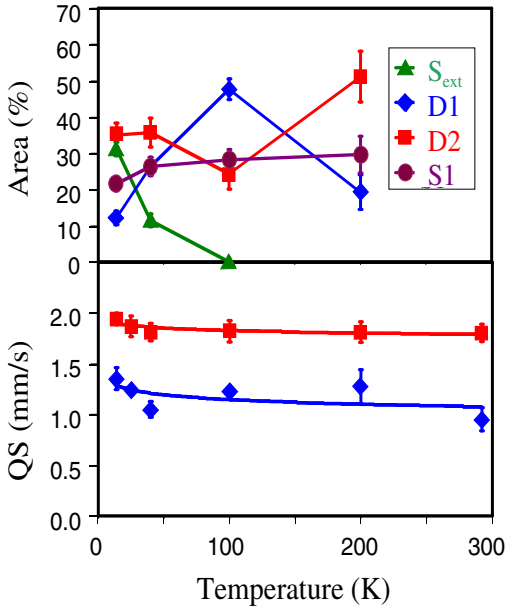

FIG. 4 (color online). Area fractions and QS ($D1$ and $D2$) obtained from Figs. 1–3 from the simultaneous fitting procedure. Area fractions are shown for the HOPG samples only since deviations might occur between oriented and polycrystalline samples. The fast drop of S_{ext} is due to the transition to $D1$; the drop of $D1$ above 100 K is attributed to a smaller Debye temperature compared to $D2$ and $S1$, see explanation in Table I.

topological defects, the damage cascade will also introduce electronic disorder. Such disorder might lead to a mixture of sp^2- and sp^3-hybridized atoms cross-linking graphene layers and under certain conditions may constitute a spin system capable of forming an exchange coupled ordered state [5,23]. The coupling of ^{57}Fe to topological and/or spin defects then appears as a possible mechanism to establish the observed magnetism.

Remarkable is that magnetism only occurs in HOPG material. It is not clear whether a local damage cascade inducing the magnetic effects could be influenced by the long range order of the crystallites' orientation. One distinguishing aspect of the HOPG crystals is, however, that they are derived from materials in a pyrolytic process at very high temperatures from which a high number of unpaired spins result [2]. These spins might be part of an exchange interaction with defects and/or hydrogen also coupling with Fe.

While the evidence given points to an ordered magnetic state at the probe atom, one also has to consider the possibility that the magnetically split spectrum might be obtained by a paramagnetic state with long relaxation time $\tau_{\mathrm{Rel}} > \hbar/A$ where A is the hyperfine interaction constant. Such paramagnetic ions are well known to occur in certain materials and molecules in which they are present as ferric Fe, Fe^{III} [24]. This then implies that Fe has a half-filled d-shell, and the ion is in an $L = 0$ state without orbital contribution to the total spin, suppressing spin-lattice relaxation. $D1$ as $Fe^{(II)}$, however, has orbital contribution to the total spin, and a short relaxation time is expected which from all literature evidence does not lead to a paramagnetically split spectrum without external magnetic field [25]. The temperature dependence measured between 14 and 40 K supports the interpretation as an ordered magnetic state: a paramagnetic state with long τ_{Rel} would keep the orientation of the atomic spin leading to magnetism at the nucleus constant over the lifetime of the Mössbauer state; no temperature dependence of B_{hf} would be expected. Then, with decreasing τ_{Rel} approaching $\hbar/A$, a relaxational spectrum with line broadening and changes of the spectral shape would result. This is not seen in either spectrum at 14 or 40 K; instead, a 10% change in B_{hf} within the 25 K interval is seen at constant line width allowing a rough estimate of the ordering temperature—assuming a Brillouin-type temperature dependence: it should be below 100 K, in agreement with the data.

To conclude, about 35% of single Fe atoms implanted in HOPG experience a magnetic hyperfine field B_{hf} of 32.6 T at 14 K. This field exists up to about 40 K. This is the first time atomic scale information is obtained on the formation of magnetism in the nominally diamagnetic graphite. A correlation of the probe atom's structural site with the electronic properties is observed. Tentative interpretations are presented that implantation-induced paramagnetic lattice defects, unpaired spins, and/or a mixture of sp^2 and sp^3 bonded carbon atoms may lead to a magnetic moment structure dense enough to allow exchange interaction with the local Fe moment.

We thank W. Bohne, J. Röhrich, and K. Potzger for their help.

[1] C. Liu *et al.*, J. Mater. Sci.: Mater. Electron. **16**, 555 (2005).
[2] T. L. Makarova, Semiconductors **38**, 615 (2004).
[3] P. Esquinazi *et al.*, Phys. Rev. Lett. **91**, 227201 (2003); P. Esquinazi *et al.*, Carbon **42**, 1213 (2004).
[4] P. O. Lehtinen *et al.*, Phys. Rev. Lett. **93**, 187202 (2004).
[5] J. Gonzalez *et al.*, Phys. Rev. B **63**, 134421 (2001).
[6] J. M. D. Coey *et al.*, Nature (London) **420**, 156 (2002).
[7] M. Venkatesan *et al.*, Nature (London) **430**, 630 (2004).
[8] Ch. Das Pemmaraju and S. Sanvito, Phys. Rev. Lett. **94**, 217205 (2005).
[9] M. De Potter *et al.*, Phys. Lett. A **97**, 404 (1983).
[10] G. D. Sprouse *et al.*, in *Mössbauer Effect Methodology*, edited by I. J. Gruverman (Plenum, New York, 1968), Vol. 4.
[11] R. Sielemann and Y. Yoshida, Hyperfine Interact. **68**, 119 (1991).
[12] D. L. Williamson *et al.*, in *Hyperfine Interactions of Defects in Semiconductors*, edited by G. Langouche (Elsevier, Amsterdam, 1992), p. 1.
[13] P. Schwalbach, thesis, TH Darmstadt, 1990 Germany (unpublished).
[14] G. Weyer, Nucl. Instrum. Methods Phys. Res. **186**, 201 (1981).
[15] V. I. Goldanskii *et al.*, Phys. Lett. **3**, 344 (1963).
[16] Data handling destroyed part of the spectra in which the absence of magnetically split lines had been realized by inspection. Notes given in the experimenters' logbook June 2006, HMI Berlin, Germany.
[17] N. N. Greenwood and T. C. Gibb, *Mössbauer Spectroscopy* (Chapman and Hall, London, 1971), p. 91.
[18] J. Kuebler *et al.*, Z. Phys. B **92**, 155 (1993).
[19] W. Bohne *et al.*, Nucl. Instrum. Methods Phys. Res., Sect. B **136-138**, 633 (1998).
[20] M. Menningen *et al.*, Phys. Lett. A **77**, 455 (1980).
[21] J. Osorio-Guillen *et al.*, Phys. Rev. Lett. **96**, 107203 (2006).
[22] G. Bouzerar and T. Ziman, Phys. Rev. Lett. **96**, 207602 (2006).
[23] A. A. Ovchinnikov and L. I. Shamovsky, THEOCHEM **251**, 133 (1991).
[24] V. I. Goldanskii and E. F. Makarov, in *Chemical Applications of Mössbauer Spectroscopy*, edited by V. I. Goldanskii and R. H. Herber (Academic Press, New York and London, 1968), p. 86 and references therein.
[25] H. H. Wickman and G. K. Wertheim, in *Chemical Applications of Mössbauer Spectroscopy*, edited by V. I. Goldanskii and R. H. Herber (Academic Press, New York and London, 1968), p. 548.